Development of high-strength corrosion-resistant austenitic TWIP steel

L. Mujica, S. Weber, W. Theisen

Based on thermodynamic calculations a (C+N) TWIP steel with the nominal composition Fe-25Mn-12Cr-0.3C-0.4N was developed and produced. Casting, diffusion annealing, hot rolling and water quenching were performed leading to a fully austenitic structure without δ-ferrite or ε-martensite. Unidirectional tensile tests were performed, revealing a yield strength of 460 MPa, ultimate tensile strength of 880 MPa (1700 MPa true strength) and an engineering strain of up to 100% at room temperature. The plasticity mechanisms were analysed based on the results of the tensile tests and cold work hardening behaviour, accompanied by microstructural analyses on deformed samples using X-Ray diffraction. Twinning was found to be an important deformation mechanism, while martensitic transformations do not take place in these materials. Correlation with predicted values of stacking fault energy (SFE) based on thermodynamic modelling is also taken into account. Electrochemical corrosion tests show a good extent of passivation in 0.5 M H_2SO_4 electrolyte. The structure, mechanical properties and corrosion resistance are compared to conventional TWIP steels such as Fe-25Mn-3Al-3Si and Fe-22Mn-0.6C.

Keywords:
TWIP steel, corrosion resistance, C+N steels, high strength steel, thermodynamic equilibrium calculations

INTRODUCTION

In the automotive industry, steels combining high strength and deformability are requested for instance to ensure future safety requirements. Under mechanical load, certain high-Mn austenitic steels exhibit high strength and exceptional plasticity due to the formation of twins in the austenitic (fcc) matrix, known as Twinning Induced Plasticity effect (TWIP) or are able to transform the austenite into ε- or α-martensite, designated as Transformation Induced Plasticity effect (TRIP). Typical TWIP steel systems are Fe-Mn-C or Fe-Mn-Al-Si. One of the disadvantages of these alloys is a low corrosion resistance.

The present study is focused on the design of high-strength, corrosion resistant TWIP steels, based on thermodynamic calculations. The element manganese is used as austenite stabilizer and to provide the induced plasticity effect. Chromium is used in order provide solubility of nitrogen in the melt and improve the corrosion resistance of the material. Carbon and nitrogen are used as interstitials to increase strength and stabilize the austenitic phase. Nitrogen has the additional effect of improving the corrosion resistance of the steel. The total interstitial content (C+N) and the C to N ratio (C/N) are critical parameters in order to ensure primary austenitic solidification, avoid gasification during casting at atmospheric pressure and avoid the formation of δ-ferrite.

Mechanical tests, microstructural characterization and analyses of deformed samples using X-Ray diffraction, correlation with calculated values of stacking fault energy (SFE) and electrochemical corrosion tests were performed to characterize the developed material. Finally, the results are compared to conventional TWIP steels such as Fe-25Mn-3Al-3Si and Fe-22Mn-0.6C.

Lais Mujica
Lehrstuhl Werkstofftechnik, Ruhr-Universität Bochum
Max-Planck Institut für Eisenforschung

Sebastian Weber
Lehrstuhl Werkstofftechnik, Ruhr-Universität Bochum
Helmholtz-Zentrum Berlin für Materialien und Energie GmbH

Werner Theisen
Lehrstuhl Werkstofftechnik, Ruhr-Universität Bochum

Paper presented at the 2nd International Conference on Super High Strength Steels, Peschiera del Garda, 16-20 October 2010, organized by AIM

MATERIALS AND METHODS

The construction of the phase diagrams was performed by Thermo-Calc® software, with the database TCFE5.

Based on the results of the thermodynamic calculations, the melting and thermo-mechanical processing of the alloy was performed. Electrolytic manganese, chromium nitride, graphite and iron were used as raw materials for the melt. A 1 kg ingot of 28 mm diameter was produced at a nitrogen partial pressure of 900 mbar. Afterwards the bar was hot forged to 14 mm in diameter, diffusion annealed at 1200°C in nitrogen atmosphere for 16 h and quenched in water.

The microstructure of the steel bar in the undeformed state was characterized by means of scanning electron microscopy (SEM). The SEM was equipped with a tungsten filament. The samples were prepared by grinding and mechanical polishing with diamond paste from 6μm, 3μm and 1μm down to 0.05 μm using colloidal silica. Electron backscattered contrast as well as secondary electron imaging was used in order to reveal the microstructure.

Tensile tests according to the standard DIN 50125 D4x20 were performed. The tests were carried out at constant strain rate of $1x10^{-3}$ s^{-1} at room temperature. Additional samples were deformed to 10% and 20% engineering strain for further XRD analyses. For these analyses, samples in the direction of the load and in transverse direction were taken with electrospark cutting.

The samples were ground and mechanically polished to submicron size. Electropolishing was used to remove any possible surface distortion formed during mechanical preparation, carried out with Struers A2 solution (perchloric acid/ethanol/2-Butoxyethanol/water).
Stacking fault energy was measured by TEM with the extended triple node method in collaboration with the Kurdyumov Institute for Metal Physics (Kiev, Ukraine)
X-ray diffraction measurements were carried out on the same samples in order to verify the formation of α- or ε- martensite due to the deformation. A Cobalt anode was used with a beam diameter of 1.5 mm.
Linear polarization curves were obtained using a PGP201 galvanostat/potentiostat, a saturated calomel as reference electrode, platinum as counter electrode and using 0.5 M H_2SO_4 as electrolyte.

RESULTS AND DISCUSSION

Thermodynamic equilibrium calculations

The thermodynamic calculations were performed under two conditions. Setting a minimum content of 12 wt-% Cr as a parameter in the steel to provide corrosion resistance and 1 bar as pressure for the production of the alloy at atmospheric condition. Based on previous studies concerning the role of the C/N ratio of the stability of the austenitic phase field in relation to nitrogen solubility as well as carbide and nitride precipitation [1,2], a C/N ratio of 0.75 was chosen for the production of the steel.
In Figure 1 the phase diagram at 1 bar of absolute pressure of a Fe-25Mn-12Cr (C/N) 0.75 alloy is depicted. The most important phase transitions correspond to liquid (L) => liquid + austenite (L+A) and liquid + austenite (L+A) => austenite (A). A direct transition of these three phases in the range of a total interstitial content between 0.6 and 0.85 mass% is clearly seen. A total interstitial content of 0.7 mass% at a C/N ratio of 0.75 was chosen to avoid primary ferritic solidification. In the case of a ferritic solidification, due to the low nitrogen solubility in ferrite, the nitrogen dissolved in the liquid matrix could be released from the freshly formed crystalline bcc structures, modifying the intended nitrogen content of the solid matrix and leading to defects such as pores. An interstitial content higher than 0.85 mass% is not contemplated due to the finite solubility in the liquid state.
In Figure 2 the microstructure of the Fe-25Mn-12Cr-0.3C-0.4N steel is depicted. No δ-ferrite was detected, being a result of the direct austenitic solidification. Neither ε-martensite was encountered, a phase that is commonly found in manganese steels with a relatively low interstitial content not high enough to stabilize the austenitic matrix. ε-martensite can also be formed as an effect of strain induced transformation.
Another remarkable effect of the microstructure is the absence of pores associated to nitrogen degassing during solidification, being a very positive effect for the manufacturing at atmospheric pressure. Nevertheless, the presence of manganese oxides is perceptible, being an effect of the manganese oxidation before solidification and appearing as small inclusions in the grains.

Strength and deformation mechanisms

The results of the uniaxial tensile tests of Fe-25Mn-12Cr-0.3C-0.4N at room temperature are presented in the Figure 3 and Table 1. In comparison, values of two common TWIP materials are given. The yield strength of the alloy Fe-25Mn-12Cr-0.3C-0.4N is higher due to the effect of solid solution strengthening of carbon and nitrogen, having a total interstitial content of 0.7 mass-%. The steel Fe-22Mn-0.6C exhibits yield strength similar to that of the developed alloy, being just slightly reduced due to

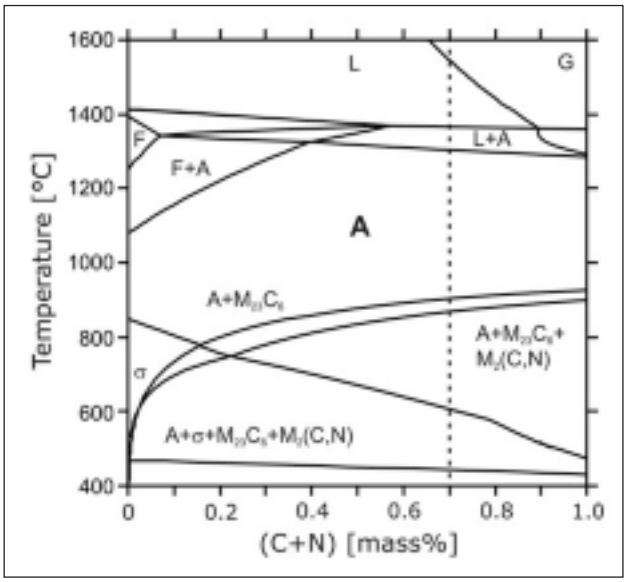

FIG. 1 ***Phase diagram of the system Fe-20Mn-12Cr-C-N (C/N=0.75).***

Diagramma di fase del sistema Fe-20Mn-12Cr-C-N (C/N=0.75).

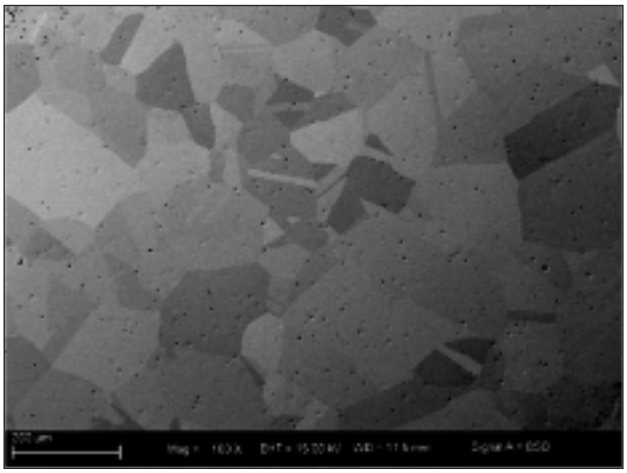

FIG. 2 ***Microstructure of the steel Fe-25Mn-12Cr-0.3C-0.4N.***

Miscrostruttura dell'acciaio Fe-25Mn-12Cr-0.3C-0.4N.

a lower interstitial content. The alloy Fe-25Mn-3Al-3Si has the lowest value, due to the absence of interstitials. The three presented steels have a large extent of deformation and cold work hardening as well as a high toughness.
From regression of the experimental tensile curve the coefficients of the Ludwigson [5] equation were determined:

$$\sigma = K_1 \varepsilon^{n_1} + e^{K_2} \varepsilon^{n_2} \quad (1)$$

The coefficients are used for the analysis of the cold work hardening of austenitic steels. The first group of terms describes the linear strengthening at high strains, while the second group is related to the work hardening at lower strains. Similar values have been reported for manganese austenites containing carbon, nitrogen or the combination of both as interstitials [6]. The value of the strain hardening exponent n_1 is indicative of an intensive cold work hardening. The strength coefficient, K_1 is related to the interstitial content. The exponent n_2 has a very low value, therefore the last group of terms can be associated to the yield strength.

Steel	$Rp_{0.2}$ [MPa]	R_m [MPa]	R [MPa]	A [%]
Fe-25Mn-12Cr-0.3C-0.4N	460.8	880.2	1702.4	100.8
Fe-25Mn-3Al-3Si (a)	250	920	1656	95
Fe-22Mn-0.6C (b)	440	1000	1700	70

TAB. 1
Tensile properties of the developed alloy in comparison with two conventional TWIP steels. (a) Frommeyer 2003, (b) Barbier 2009.

Caratteristiche di resistenza a trazione della lega sviluppata confrontata con due acciai TWIP convenzionali. a) Frommeyer 2003, (b) Barbier 2009.

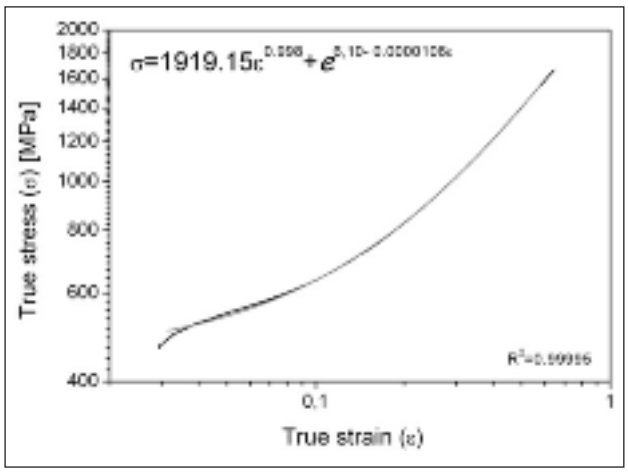

FIG. 3 ***True stress- true strain diagram of the Fe-25Mn-0.3C-0.4N. The black line represents the measured data and the grey line the fitted line according to Ludwigson relation. The equation corresponds to the regression from the Ludwigson relation.***

Diagramma carico effettivo –deformazione effettiva dell'acciaio Fe-25Mn-0.3C-0.4N. La linea nera rappresenta i dati misurati e la linea grigia rappresenta la linea secondo la relazione di Ludwigson. L'equazione corrisponde alla regressione dalla relazione di Ludwigson.

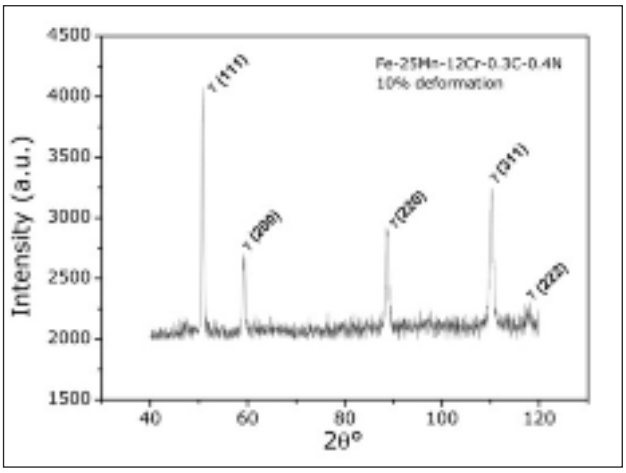

FIG. 4 ***XRD Spectrum of the steel Fe-25Mn-12Cr-0.3C-0.4N after 10% plastic deformation.***

Spettro XRD dell'acciaio Fe-25Mn-12Cr-0.3C-0.4N dopo deformazione plastica del 10%.

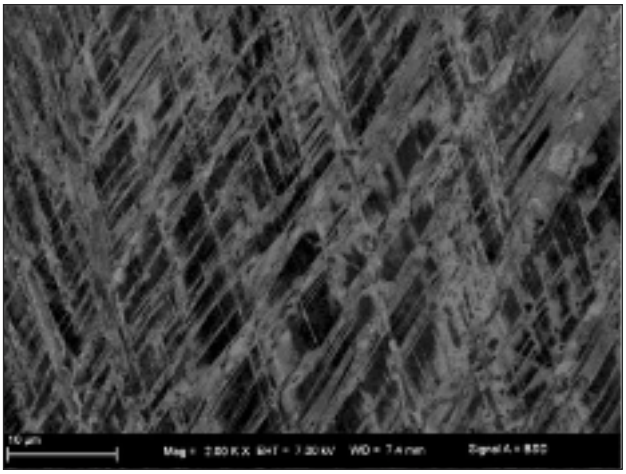

FIG. 5 ***SEM back scattered image of the deformed microstructure of the steel Fe-25Mn-12Cr-0.3C-0.4N after fracture.***

Immagine SEM con elettroni retrodiffusi della microstruttura deformata dell'acciaio Fe-25Mn-12Cr-0.3C-0.4N dopo rottura.

X-Ray diffraction measurements were performed to find out the deformation mechanism and if the large extent of plastic deformation was related to a phase transformation or not. From a tensile test specimen of Fe-25Mn-12Cr-0.3C-0.4N after 10% of plastic deformation a sample was taken. The results show no evidence for strain induced ε-martensite or α-martensite transformation. (Figure 4), being a good result of the stability of the austenitic structure.

The stability in this case can be related to an interstitial content high enough to prevent transformations induced by thermal processes (water quenching) as in the case of Fe-26Mn-0.16C [7] and Fe-Mn systems [8], or by strain, as the well known TRIP steels [3].

The characterization of the microstructure of a plastically deformed sample reveals mechanical twins, as shown in Figure 5, where two different twin systems intersect. The thickness of the twins varies from submicron size to ~ 4μm, where the thick twins consist of groups of thinner twins packed close to each other.

The fact that the developed steel has as interstitial elements carbon and nitrogen, can have an influence in relation to the deformation mechanism. The role of carbon and nitrogen in the cold work hardening behaviour has to be considered, too. It has been proposed, that carbon produces a strong elastic interaction with dislocations, having as an effect the hindering of dislocation slip and promoting twinning, such as in the case of Hadfield steel [6]. In nitrogen alloyed steels, it is proposed as intersection of planar slip bands forming Lomer-Cottrell junctions [6], that is, sessile dislocations creating a barrier where following dislocations pile-up, where the sessile dislocations are formed from Shockley partial dislocations.

It should be noticed, that the motion of Shockley partial dislocations generates stacking faults in the (111) close packed planes in austenite as well [9]. This kind of dislocations participates in different strengthening mechanisms of the manganese ste-

Steel	SFE [mJ/m²]
Fe-25Mn-12Cr-0.3C-0.4N	31(a)
Fe-25Mn-3Al-3Si	25 (b)
Fe-22Mn-0.6C	20 - 22(c)

Tab. 2 ***Comparison of the SFE and free Gibbs energy of the transformation. (a) Measured value. (b) According to Frommeyer (2003). (c) According to Allain (2004), Saeed-Akbari (2009), Petrov 2005.***

Confronto fra SFE-energia di stacking fault ed energia libera di Gibbs della trasformazione. (a) Valore misurato. (b) Secondo Frommeyer (2003). (c) Secondo Allain (2004), Saeed-Akbari (2009), Petrov 2005.

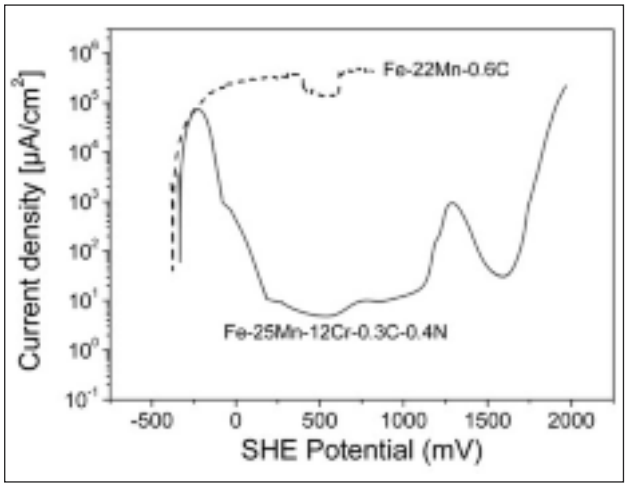

FIG. 6 ***Current potential diagram of the steels Fe-25Mn-12Cr-0.3C-0.4N and Fe-22Mn-0.6C in 0.5M H_2SO_4 solution [2].***

Diagramma corrente-potenziale degli acciai Fe-25Mn-12Cr-0.3C-0.4N e Fe-22Mn-0.6C in soluzione 0.5M H_2SO_4 [2].

els, creating ε-martensite embryos, twin embryos and the Lomer-Cottrell locks. The presence of one or more mechanisms will depend mainly on the alloy constitution and would be reflected in the stacking fault energy values as well.

It is known that the induced plastic deformation substructures (ε-martensite and twins) are associated with manganese as austenite former, being a common element of the developed and the reference steels. The measured stacking fault energy of Fe-25Mn-12Cr-0.3C-0.4N steel in comparison to the reference TWIP steels is presented in Table 2. The value is higher than that of the reference steels, however, it is in the range of SFE where twinning as predominant deformation mechanism can be expected. The presence of interstitials in the alloy, and moreover, a combination of carbon and nitrogen, has an effect on the stacking fault energy. This effect is proposed to be related to a change in the free-electron concentration [12, 13]. According to those works, carbon weakly increases the free-electron concentration (~$0.25x10^{22}$ electrons/cm³), nitrogen increases this value more significantly (0.5-$1.25x10^{22}$ electrons/cm³), whereas C+N alloying increases the free electron concentration one order of magnitude (2.0-$3.75x10^{22}$ electrons/cm³). One should take into account, that the dependence of SFE on the interstitial content is non-monotonic and depends on the elements occupying the substitutional sites, like Mn, Cr, Fe, or Ni.

Corrosion resistance

Previous corrosion investigations made of the system Fe-Mn-Al-Si [15] reveals poor corrosion resistance in 0.1M H_2SO_4 acidic solution, attributed to the non-passivation tendency of aluminium in this medium, high manganese and iron dissolution in acidic medium, facilitated by hydrogen evolution reaction.

The corrosion behaviour of the developed steel was evaluated in 0.5 M H_2SO_4 electrolyte, showing remarkable differences to the Fe-Mn-C reference steel, as seen in the current density – potential diagram in Figure 6. The difference arises from the ability of chromium to build passivation layers: In case of Fe-25Mn-12Cr-0.3C-0.4N steel, there is a distinct active regime from -250 mV to +125 mV (SHE), having a critical current density of $72x10^3$ μA/cm². The passive area reaches 1250 mV, where a first breakdown potential is seen, the passive current is about 5 μA/cm². Afterwards, a second passive area is present in the range of 1125 to 1375 mV.

In contrast, the reference TWIP steel shows a significantly larger active area in terms of the range of the potentials and the height of current density. The Fe-Mn-C reference steel shows passivity, however, the current densities are in the range of $1x10^5$ μA/cm², being five orders of magnitude compared to the developed steel.

SUMMARY

A high-strength corrosion-resistant C+N austenitic TWIP steel was developed with the nominal composition Fe-25Mn-12Cr-0.3C-0.3N, leading to a new kind of material featuring an exceptional combination of strength, ductility and corrosion resistance. The XRD measurements, measured values of SFE and deformation microstructures support twinning as predominant deformation mechanism. In H_2SO_4 media, the developed steel outperforms better than the conventional TWIP steels based on the systems Fe-Mn-C or Fe-Mn-Al-Si.

ACKNOWLEDGMENTS

The authors would like to thank the contribution of the Prof Valentin Gavriljuk and Prof. Yu Petrov in the Kurdyumov Institute for Metal Physics (Kiev, Ukraine) for the measurements of the SFE.

REFERENCES

1. Mujica L., Weber S., Theisen W. Computer Assisted Development of Corrosion Resistant TWIP Steels, Proceedings of 10-th International Conference on High Nitrogen Steels (HNS 09), Edited by Svyazhin, A.G., Prokoshkina, V.G., Kossyrev, K.L., 6-8 July 2009, MISIS, Moskau, S. 306-31
2. Mujica L., Weber S., Theisen W. Development of Mn-Cr-(C-N) corrosion resistant TWIP steels: thermodynamic and diffusion calculations, production and characterization. Metallurgical and Materials Transactions A, 2010, 41A, 2471.
3. Frommeyer G, Brüx U, and Neumann P. Supra-ductile and high-strength manganese Trip/Twip steels for high energy absorption purposes. ISIJ International, Vol. 43 (2003), No. 3, 438–446.
4. Barbier, D., Gey, N., Allain, S., Bozzolo, N., Humbert, M. Analysis of the tensile behaviour of a TWIP steel based on the texture and microstructure evolutions. Materials Science and Engineering A 500 (2009) 196–206.
5. Ludwigson, D.C. Modified stress-strain relation for FCC metals and alloys. Metallurgical and Materials Transactions B, 2 (1971) 10, 2825-2828
6. Gavriljuk, V.G., Tyshchenko, A.I., Bliznuk, V.V., Yakovleva, I.L., Riedner, S. Berns, H. Cold work hardening of Hight-Strenght Austenitic Steels. Materials Technology, Steel research international 79 (2008) No. 6, 413-422.
7. P. Sahu, A. S. Hamada, S. Ghosh Chowdhury, L. P. Karjalainen. Structure and microstructure evolution during martensitic transformation in wrought Fe–26Mn–0.14C austenitic steel: an effect of cooling

rate. J. Appl. Cryst. (2007). 40, 354–361
8. Lee, Y.-K., Jun, J.-H., CHOI, C.-H. DampingCapacity in Fe-MnBinary Alloys. ISIJ Internationai, Vol. 37 (1 997), No. 10, pp. I023-1030
9. G. B. Olson M. Cohen.General Mechanism of Martensitic Nucleation: Part I. General Concepts and the FCC HCP Transformation. Metallurgical Transactions A. 7A, (1976) 1897-1904
10. Allain S, Chateau J, Bouaziz O, Migot S and Guelton N. Correlations between the calculated stacking fault energy and the plasticity mechanisms in Fe–Mn–C alloys Materials Science and Engineering A, 387–389 (2004) 158–162.
11. Saeed-Akbari, A., Imlau, J., Prahl, U., Bleck, W.. Derivation and Variation in Composition-Dependent Stacking Fault Energy Maps Based on Subregular Solution Model in High-Manganese Steels. Metallurgical and Materials Transactions A, 40 (2009) 13, 3076-3090.
12. Petrov Y. On the electron structure of Mn–, Ni– and Cr–Ni–Mn austenite with different stacking fault energy. Scripta Materialia 53(2005) 1201–1206
13. Gavriljuk V, Shanina B and Berns H. A physical concept for alloying steels with carbon + nitrogen . Materials Science and Engineering A, 481-482 (2007) 707-712
14. Gavriljuk V and Berns H. High Nitrogen Steels: Structure, properties, manufacture and applications. Berling: Springer, 1999
15. Bobby Kannan, M., Singh Raman, R. K., Khoddam, S. Comparative studies on the corrosion properties of a Fe–Mn–Al–Si steel and and interstitial-free steel. Corrosion Science 50 (2008) 2879–2884

Abstract

Sviluppo di un acciaio austenitico TWIP ad alta resistenza alla corrosione

Parole chiave: acciaio, corrosione, modellazione

Il presente lavoro prende in considerazione un acciaio TWIP (C + N) con composizione nominale Fe25-Mn-12Cr-0.3C-0.4N che è stato sviluppato e prodotto sulla base di calcoli termodinamici. Sono stati effettuati i processi di colata, ricottura di diffusione, laminazione a caldo e spegnimento in acqua che hanno permesso di ottenere una struttura completamente austenitica senza δ-ferrite o ε-martensite. Sono state eseguite prove di trazione unidirezionali, rivelando una resistenza allo snervamento di 460 MPa, un carico di rottura di 880 MPa (1700 MPa reale) e un allungamento fino al 100% a temperatura ambiente. I meccanismi di plasticità sono stati analizzati sulla base dei risultati delle prove di trazione e comportamento all'incrudimento a freddo, oltre che analisi microstrutturali su campioni deformati mediante diffrazione a raggi X. La geminazione si è dimostrata un importante meccanismo di deformazione, mentre le trasformazioni martensitiche non avvengono in questi materiali. E' stata presa in considerazione anche la correlazione con i valori previsti di energia dei difetti di impilamento (Stacking Fault Energy - SFE) basata sulla modellizzazione termodinamica. Le prove di corrosione elettrochimica mostrano una buona misura di passivazione in 0,5 M di H_2SO_4 elettrolita. La struttura, le caratteristiche meccaniche e la resistenza alla corrosione sono state confrontate con quelle dei tradizionali acciai TWIP come Fe-25Mn-3Al-3Si e Fe-22Mn-0.6C.